Scanning Microscopy

Volume 1992
Number 6 *Signal and Image Processing in Microscopy and Microanalysis*

Article 9

1992

Application of Slow-Scan Charge-Coupled Device (CCD) Cameras to On-Line Microscope Control

O. L. Krivanek
Gatan Research and Development, California

G. Y. Fan
University of California at San Diego

Scanning Microscopy Supplement 6, 1992 (pages 105-114) 0892-953X/92$5.00+.00
Scanning Microscopy International, Chicago (AMF O'Hare), IL 60666 USA

APPLICATION OF SLOW-SCAN CHARGE-COUPLED DEVICE (CCD) CAMERAS TO ON-LINE MICROSCOPE CONTROL

O.L. Krivanek* and G. Y. Fan[1]

Gatan Research and Development, 6678 Owens Drive, Pleasanton, CA 94588, USA
[1]present address: Department of Neurosciences, University of California at San Diego, La Jolla, CA 92093, USA

Abstract

Autotuning methods for transmission electron microscopy are reviewed, and a distinction is drawn between predictive and non-predictive methods. The predictive methods make better use of the input data and therefore need fewer images to carry out complete autotuning. They typically require high quality of input data, which can be best provided by cooled slow-scan charge-coupled device (CCD) cameras. Two predictive methods are considered in more detail. These are the tilt-induced image shift (TIS) method of Koster, van der Mast and de Ruijter, and a new automated diffractogram analysis (ADA) method, which is introduced in this paper. The ADA method is shown to be capable of accurately aligning, stigmating and focussing a TEM in less than 30 seconds using just three high resolution images, and of automatically calibrating all the needed microscope parameters.

Key Words: TEM autotuning, slow-scan CCD cameras, coma-free alignment, autostigmation, autofocusing, tilt-induced image shift, tilt-induced astigmatism, automated diffractogram analysis, Macintosh II and Quadra, DigitalMicrograph software.

*Address for correspondence:
Ondrej L. Krivanek
Gatan R&D
6678 Owens Drive
Pleasanton, CA 94588, USA
Telephone number: (510) 463 0200
FAX number: (510) 463 0204

Introduction

It is a curious fact that one can get an autofocusing 35-mm camera for about $100, but that until recently, even 10 000 times this amount could not procure an autofocusing transmission electron microscope (TEM), since no such instrument was commercially available. The gains brought by an autofocusing TEM should be much the same as the ones brought by an autofocusing camera: more convenient operation making life easier for the experts and enabling novices to take good pictures, higher percentage of good pictures for everybody, and shorter set-up time allowing fast-changing scenes (or specimens) to be imaged successfully.

Interest in TEM autofocusing (or more generally: autotuning) arose soon after TEM image recording devices developed to the point where a computer could be provided on-line with image data, and several systems have been put into practice [e.g., 5, 6, 7, 10, 13, 14]. The required hardware has become relatively standard: a TEM, an image recording device such as an intensified TV camera, and a computer capable of capturing and analyzing images from the recording device, and able to control the microscope. The autotuning proceeds in much the same way as when a human operator is setting up the microscope: 1) the TEM produces an image, 2) the computer captures the image, and analyzes it to gain information on an adjustment parameter (or parameters), 3) the computer changes the microscope set-up, captures another image, and performs the analysis once more, and 4) the process is repeated until all the relevant parameters are optimized.

The essential parameters are the tilt (alignment) of the illuminating beam (in x and y directions), the astigmatism (x and y), and the defocus. Compared to a human operator, the computer has the advantage that it analyzes the images quantitatively, and can therefore make better use of the input data than a human operator, who is only able to make qualitative judgments such as "this image looks sharper than the other image". On the minus side for the computer, it may not notice that anything has gone wrong, and one of the trickier tasks in writing autotuning software is building in enough safeguards to guarantee that a bad image will not be made even worse by the computer.

Early autotuning procedures [10, 13, 14] were based on image contrast as the image property used to evaluate the microscope adjustment. Because the contrast of just one image contains no clues about how much the microscope adjustment is in error, a series of typically 20 images needed to be captured while each of the 5 essential parameters was varied, i.e. a total of 100 images for complete autotuning. More recent procedures are based on image shift as a function of incident beam tilt [5, 6, 7, 16], and on defocus and astigmatism

measured from a diffractogram (this paper). They have the advantage that only a few images are needed to provide a quantitative measure of how much a parameter needs to be adjusted. This makes them better suited to operation with slow-scan CCD cameras, which provide high quality input, but would take a long time to read out the large number of images required by the contrast evaluation method.

In this paper we review the autotuning approaches already developed, and evaluate them from the perspective of using a slow-scan charge-coupled device (CCD) camera as the image detector. We then introduce a new autotuning method based on automatic diffractogram analysis, and show that it is well suited for high resolution imaging. As a final step, we go on to the considerations needed for a practical autotuning system operating on a variety of electron microscopes.

Summary of Autotuning Methods

Complete autotuning of an electron microscope consists of aligning the incident beam to be parallel to the axis of the objective lens (autoalignment), setting the astigmatism to zero (autostigmation), and setting the defocus to a user-selected value (autofocusing).

The resultant set-up of the electron microscope is characterized by the shape of its aberration function $\chi(\underline{q})$ and the direction of the incident beam. The aberration function is best pictured as a 2-dimensional surface located in the back-focal plane of the objective lens. It describes the phase shift imparted to a beam traveling at an angle θ to the optic axis of the microscope's objective lens, relative to the phase the beam had at the exit surface of the sample in the microscope.

The aberration function is given by [15]:

$$\chi(\underline{q}) = \frac{C_S \lambda^3 \underline{q}^4}{4} + \frac{(\Delta Z + A \cos 4\pi(\phi - \phi_o)) \lambda \underline{q}^2}{2} \quad [1]$$

where C_S is the coefficient of spherical aberration, λ is the electron wavelength, $\underline{q}$ is a position vector in the back-focal plane expressed in units of spatial frequency ($q = \theta/\lambda$), ΔZ is the defocus, A is the coefficient of astigmatism, ϕ is the azimuthal angle of the beam, and ϕ_o is the angle between the direction of greatest overfocus and the x-axis of the chosen coordinate system.

If the shape of the aberration function of an electron microscope and the position of its axis could be easily determined, a general-purpose autotuning procedure would probably have been worked out a long time ago. However, the phase shift of a single beam cannot be measured - only the phase difference between two or more beams can be experimentally determined. As a result, autotuning procedures have been forced to use round-about ways to measure the aberration function.

Fig. 1 illustrates the problem. It shows the aberration function of a C_S = 1 mm, 100 kV electron microscope computed for $\Delta Z = 0$, and 3 Sch (1 Sch = 1 Scherzer = $-(C_S \lambda)^{1/2}$). Only a cross-section of the 2-dimensional aberration function along the $\underline{q} = (q_x,0)$ axis is shown. (In the absence of astigmatism, other sections through the origin would look exactly the same; astigmatism would change a single section in the same way as defocus.) The function displays a characteristic form which is symmetric about the optic axis of the objective lens, and is dominated at low $|\underline{q}|$ by the defocus term, and at high $|\underline{q}|$ by the C_S term. The function itself cannot be measured, nor does one know *a-priori* the precise location of the optic axis in the back-focal plane of the objective lens. One can, however, measure the gradient of the aberration function by determining the shift of an interference pattern produced by two beams. For two beams of similar $\underline{q}$, the shift of the pattern is proportional to

$$\underline{s} \;\alpha\; (\chi(\underline{q}_2) - \chi(\underline{q}_1)) / (\underline{q}_2 - \underline{q}_1) \;\equiv\; \underline{\nabla}\chi(\underline{q}) \quad [2]$$

i.e., the shift is proportional to the gradient of the aberration function. In practice the two beams can be substituted by the low-angle scattering of say a particle, and $\underline{s}$ determines the shift of the image of the particle relative to where it would be in a perfect image. Since one does not know *a-priori* what the perfect image should look like, it is necessary to measure the shift between pairs of images taken with different beam tilt, astigmatism, or defocus settings.

Equation [2] provides the basis for the tilt-induced image shift (TIS) autotuning method [5, 6, 7, 16], which is illustrated in Figure 1 (b) and (c). (b) shows the gradient of the aberration function shown in Fig. 1 (a), which cannot be measured directly, and a mistilt $\underline{m}$ of the incident beam relative to the optic axis ($\underline{m} = (m_x,m_y)$). Zero mistilt would mean that the beam is correctly aligned according to the so-called coma-free criterion [17], and one of the tasks of the autotuning is to work out what $\underline{m}$ is. (c) shows the shift of the image of the particle when the beam is further tilted by an additional tilt $\underline{t}$ ($\underline{t} = (t_x,t_y)$) with respect to $\underline{m}$. The shift depends on both the defocus and the beam tilt. If the microscope C_S, magnification, and the calibration of the computer control of the beam tilt are all known, images taken for three different beam tilts along the q_x direction are sufficient, in principle, to determine and correct m_x, and further two images taken with different beam tilts along the q_y direction are sufficient to correct m_y. If the computer controls of the stigmator and objective lens focus have been calibrated, astigmatism and defocus can be determined at the same time from 3 of the 5 images.

The full calibration of the computer control strengths can be quite tedious. Another problem with the above approach is that in order to separate the effect of the beam tilt from the effect of defocus and astigmatism, relatively large tilt angles need to be used. Use of such angles may cause substantial changes in image appearance, making it difficult to determine the image shift accurately.

Fortunately, the TIS method can be simplified so that it does not need a detailed prior knowledge of the microscope properties, but instead automatically provides the necessary calibrations. Such a TIS method has recently been introduced by Koster and de Ruijter [6]. Using their approach but slightly different notation, the image shift can be written as:

$$\underline{d} = [f\mathbf{F} + g\mathbf{G} + h\mathbf{H} + \mathbf{R}] \; (\underline{t} - \underline{t}_c) \quad [3]$$

where $\underline{d}$ is the image shift in pixels, f denotes the computer-generated DAC (digital-to-analog converter) output controlling the objective lens current; g and h denote the computer outputs controlling the stigmator currents; **F**, **G**, and **H** are 2x2 calibration matrices describing the effect of computer adjustments on the image shift; **R** is a 2x2 matrix describing residual terms that arise because zero defocus and astigmatism typically correspond to finite values of f, g, and h; $\underline{t} = (t_x, t_y)$ is a tilt vector expressed in computer-control coordinates; and $\underline{t}_c$ is a vector describing the t_x and t_y values needed to have the beam aligned on the objective lens current center.

The simplified TIS method assumes a linear relationship between $\underline{d}$ and $\underline{t}$, and thus requires that the tilt be kept small, so that the autotuning does not step outside the linear part of the gradient of the aberration function (Fig. 1c), in which the influence of C_S is minimal. This means that coma-free alignment, which depends on experimentally determining the influence of C_S on the imaging process, cannot be worked out using this approach. However, the approach can be used to work out the current center, by determining the image shift due

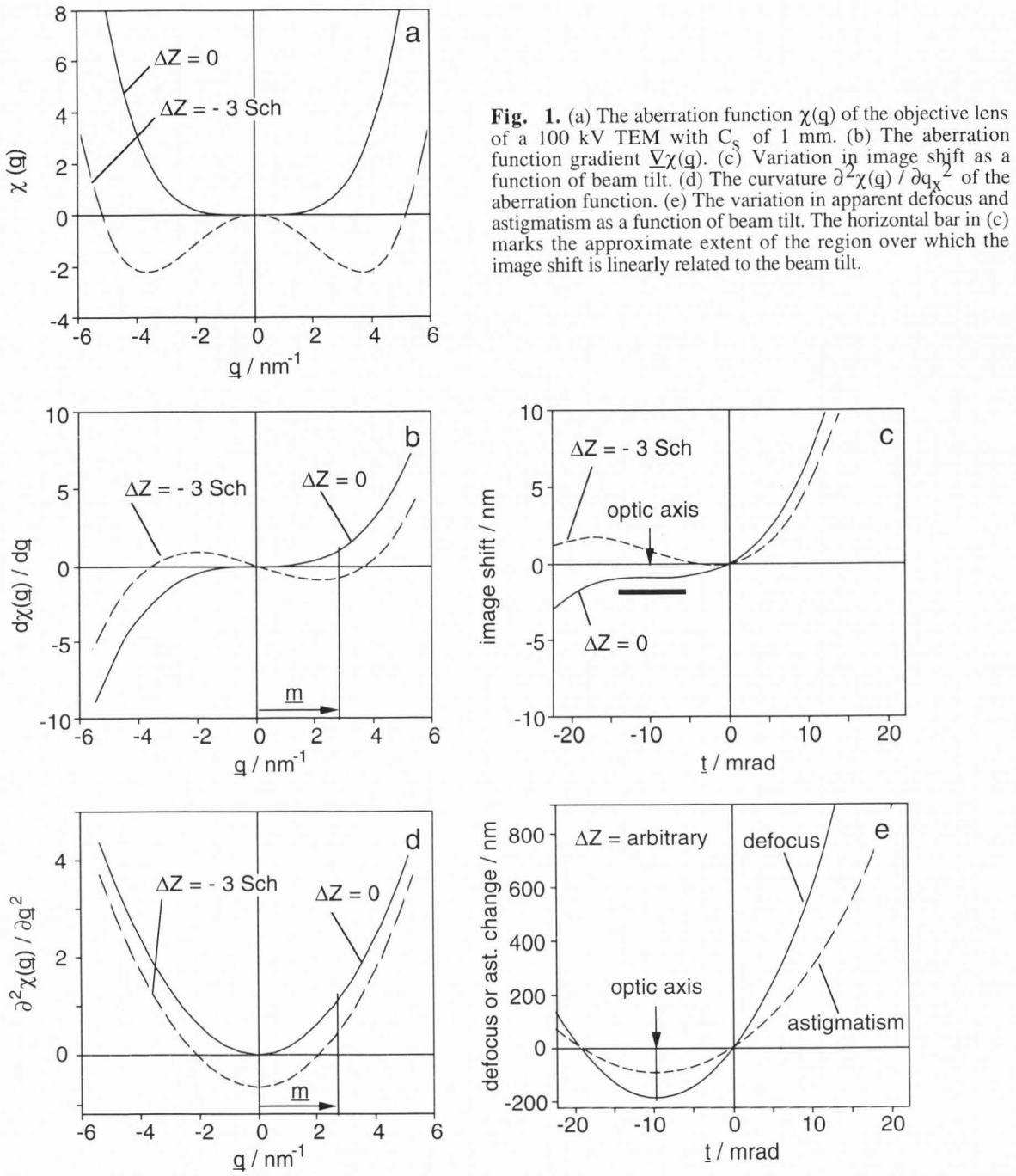

Fig. 1. (a) The aberration function $\chi(\underline{g})$ of the objective lens of a 100 kV TEM with C_S of 1 mm. (b) The aberration function gradient $\underline{\nabla}\chi(\underline{g})$. (c) Variation in image shift as a function of beam tilt. (d) The curvature $\partial^2\chi(\underline{g}) / \partial q_x^2$ of the aberration function. (e) The variation in apparent defocus and astigmatism as a function of beam tilt. The horizontal bar in (c) marks the approximate extent of the region over which the image shift is linearly related to the beam tilt.

to a change in the defocus setting f, or the voltage center, by determining the image shift due to a small change in the high voltage. A more involved, non-linear variety of TIS can determine the coma-free axis [6]. However, because current or voltage centering is typically adequate at the low and medium magnifications for which TIS is especially well suited (see below), the non-linear TIS method is likely to be less useful in practice than the simplified linear one.

A practical autotuning procedure based on the simplified TIS method is described in the next section. Our experience with it so far is that it works well with both amplitude and phase objects containing sharp distinct features, at low and medium magnification, and that it is relatively robust, since the image shift can be measured even when the microscope is a long way away from correct set-up. The method does not work well when the image structure changes with the beam tilt so much that determining the exact image shift becomes impossible, for instance at high magnification when the specimen does not have any distinct features such as small particles. Further disadvantages are that the results are thrown off by specimen drift, and by spurious image shifts produced by a small part of the magnetic field of the beam tilting coil penetrating below the sample. The last problem can be severe on top-entry microscopes whose objective lens has a large

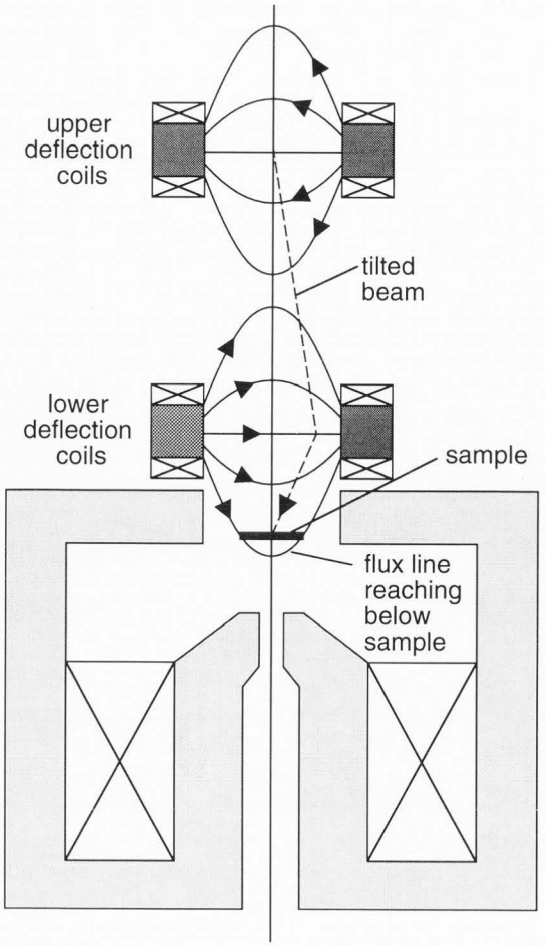

Fig. 2. Schematic diagram showing how the magnetic field of the beam tilting coils can penetrate below the specimen, thereby causing spurious image deflection when the illumination is tilted.

upper bore diameter, and whose bottom beam-tilting coils are situated just above the objective lens (Fig. 2). It means that each time the beam is tilted, there is an extra shift of the image which is not related to the gradient of the aberration function. The extra shift prevents the defocus from being determined accurately. On microscopes suffering from this problem, it is important to follow the TIS autotuning procedure by a final step, in which the defocus is worked out from the image contrast, rather than from image shift.

Another property of the aberration function that can be measured is the second-order gradient (curvature) of the function ($\partial^2\chi(\underline{q}) / \partial q_x^2$, $\partial^2\chi(\underline{q}) / \partial q_y^2$). The curvature can be worked out by determining the defocus and astigmatism from the diffractogram of an electron micrograph of an amorphous material [8].

It is important to realize that the astigmatism and defocus determined by diffractogram analysis depend only on the curvature of $\chi(\underline{q})$ at the location $\underline{q} = \underline{m} / \lambda$, where $\underline{m}$ is the mistilt of the incident beam with respect to the coma-free axis. Because the curvature changes for different values of $\underline{m}$, the astigmatism and defocus appear to change with $\underline{m}$. This leads to the concept of "apparent" defocus and astigmatism [9], whereby the defocus determined by diffractogram analysis is an apparent defocus ΔZ composed of two terms: real defocus $\Delta Z'$, and tilt-induced defocus $\Delta Z''$. $\Delta Z'$ depends on the specimen height and the currents of the microscope lenses. It corresponds to the defocus that would be obtained if the illumination was precisely aligned on the coma-free axis of the objective lens. $\Delta Z''$ depends on the tilt $\underline{m}$ of of the illuminating beam with respect to the optic axis. Similarly, apparent astigmatism is the sum of real astigmatism A', which depends on the non-roundness of the objective lens and the stigmator currents, and of tilt-induced astigmatism A", which depends on $\underline{m}$.

The tilt-induced defocus and astigmatism are given by [9]:

$$\Delta Z'' = 2\, C_S\, (\underline{t} + \underline{m})^2 \qquad [4a]$$

$$A'' = C_S\, (\underline{t} + \underline{m})^2 \qquad [4b]$$

where $\underline{t}$ is an intentional tilt of the illuminating beam expressed in radians, $\underline{m}$ the starting misalignment also in radians, and the orientation of the tilt-induced astigmatism is such that the largest overfocus occurs in the direction of ($\underline{t}$ + $\underline{m}$).

The relationship between the second-order curvature and the tilt-induced defocus and astigmatism is illustrated in Fig. 1 (d) and (e). (d) shows the curvature of the aberration function of Fig. 1 (a). (e) shows the variations of apparent defocus and astigmatism when the illuminating beam is tilted by an additional tilt $\underline{t}$ with respect to $\underline{m}$. The resultant curves are parabolas independent of the real defocus $\Delta Z'$ and of real astigmatism A'. If C_S, the microscope magnification, and the magnitude of the additional beam tilt are known, images taken for just two different beam tilts are sufficient to determine the misalignment $\underline{m}$. The real defocus and astigmatism can be determined at the same time from one of the two images by analyzing its diffractogram, and making a correction for the tilt-induced defocus and astigmatism.

An autoalignment method based on the above arguments could use the tilt-induced defocus change, but it is more advantageous to use the tilt-induced astigmatism A". This is because A" carries directional information which enables one to determine the mistilt in both the x and y directions while tilting the illumination in only one direction. Another advantage of the tilt-induced astigmatism approach is that unlike defocus, astigmatism is insensitive to instabilities in the high voltage and the objective lens current. In adding any two astigmatism values, such as A' and A", however, one must be careful to take into account that astigmatism is 2-fold symmetric, meaning that a rotation by 180° brings it back to the original value, and a rotation by 90° just reverses its polarity. A practical way to deal with this complication is to introduce an astigmatism vector $\underline{A}$, whose magnitude is equal to A, and which points in a direction given by 2 ϕ_O, where ϕ_O is the angle between the direction of the largest overfocus and the x-axis of the coordinate system. It further turns out that because a rotation can be expressed simply as a multiplication of two complex numbers, it is convenient to represent the vector $\underline{A}$ as a complex number $A = A_x + i\, A_y$.

An autoalignment procedure based on the tilt-induced astigmatism (TIA) analysis requires that an automatic determination of the astigmatism be possible. In our approach, the astigmatism is determined by automatic diffractogram analysis (ADA). The ADA method leads to complete autotuning in which the autoalignment part is carried out by combining TIA with ADA, and the autostigmation and autofocusing parts are based on ADA alone.

An ADA procedure which yields both the defocus and astigmatism has been described by us previously [3]. Briefly, the procedure divides an experimental diffractogram into 32 azimuthal segments (i.e., each segment spans 11.25°), and integrates the intensity in each segment to obtain experimental diffractogram profiles for different directions. The profiles are

weighted to increase the intensity at higher spatial frequencies, and each one is cross-correlated with an array of theoretical diffractogram profiles worked out for a range of defocus values. The cross-correlation maximum indicates the value of the defocus appropriate to each azimuthal segment. The defocus values for all the segments are then fitted to a sinusoidal variation of defocus versus azimuthal angle. This gives the apparent defocus, the apparent astigmatism, and the astigmatism direction. Finally the deviations of the defocus values of the individual segments relative to the fitted values are analyzed to give the standard variation of the fit, which is used to judge the quality of the analysis. The procedure has been found to work reliably for diffractograms containing at least 2 distinct rings. Its precision is largely determined by the quality of the input data, and is typically better than 3 nm for the defocus determination, and better than 1 nm for the astigmatism determination (the method is more accurate in detecting defocus differences rather than the absolute defocus value, which is why it determines astigmatism more accurately than defocus).

Similar to the way the simplified TIS autotuning method can be made self-calibrating, our TIA autoalignment method can also be carried out without complete prior knowledge of the microscope parameters. We write:

$$A = g\,G + h\,H + (t+m)^2\,T + R \qquad [5]$$

where *italics* represent complex numbers; g and h describe the computer outputs to the stigmators; G and H are vectors in the complex plane describing the effective strength and the direction of the stigmator coils; $t = t_x + it_y$ describes the computer-induced tilt; $m = m_x + im_y$ is the initial misalignment relative to the coma-free axis; T describes the effect of the tilt coils; and R is the residual astigmatism. Note that $(t + m)^2$ is a vector in the complex plane of magnitude equal to $|t + m|^2$, and an angle to the x-axis equal to twice the angle of $(\underline{t} + \underline{m})$, exactly as required.

Equation [5] leads to a practical autoalignment method which uses 3 images to determine the location of the coma-free axis, as described in the next section. Astigmatism and defocus are determined at the same time from one of the 3 images.

Comparing equations [5] and [3] makes it clear that, provided that an automated diffractogram analysis routine is available, full ADA autotuning is easier to implement than the simplified TIS autotuning (which does not do proper autoalignment). Whereas the instrumental calibration for TIS autotuning consists of determining four (2x2) matrices (**F**, **G**, **H** and **R**), the calibration for ADA autotuning consists of determining just four vectors. Further, if one makes a particular choice of the tilt values used by the TIA procedure, T and R drop out (see next section). This reduces the ADA calibration requirements to the determination of just 2 vectors (G and H), and a calibration of the defocus DAC. The diffractogram analysis routine also needs to know the magnification, with an accuracy of a few percent.

Further advantages of ADA autotuning are: it requires the smallest number of micrographs of all the presently known autotuning methods, it works well with the ubiquitous amorphous carbon support film, it is not perturbed by small amounts of specimen drift, changes in the high voltage and objective lens current of the microscope, or by spurious tilt-induced image shifts (all of which cause errors with TIS), and it is so simple computationally that it can be carried out in reasonable time by a high-end personal computer without an array processor. Most important for high resolution imaging, the autoalignment part of ADA works out the true center of the aberration function, as needed for coma-free alignment. The disadvantages of ADA autotuning are that it needs both the starting conditions and the image recording device to be good enough to produce diffractograms with at least two rings, and that it does not work well with crystalline materials or small particles. The method places high demands on the image recording device which are difficult to meet with TV-rate cameras [Saxton, private communication], but can be readily fulfilled with slow-scan CCD cameras.

Both the TIS and ADA methods are predictive in the sense that they predict the optimum condition of the microscope by analyzing its initial condition. They are able to do this because they use **vectorial information** (image shift and astigmatism respectively) to derive both the magnitude and the direction of the needed adjustment. By comparison, the more traditional autotuning methods use a **scalar parameter** (image contrast) to characterize the microscope condition. They find the optimum condition by locating the center of a parabolic dependence of the contrast on the adjusted parameter, and need to explore many different microscope conditions on both sides of the optimum. In other words, they need to pass through the optimum in order to recognize it. They can therefore be called non-predictive.

The simple use of the input data by the non-predictive methods is inefficient. As a consequence, they require higher doses than the predictive methods [7], and take much longer when using the same computing power. At low to medium magnification, the non-predictive methods are therefore likely to be replaced by TIS autotuning, and at high magnification by ADA autotuning. The only exception will probably occur in imaging of mixed amplitude-phase objects such as stained biological sections, for which it is not easy to predict the optimum defocus theoretically, and analyzing actual image contrast is therefore likely to lead to a better image. In this case, however, we have found that it is better to maximize image sharpness worked out by convolving the image with an edge-detecting filter (similar to recent work of Nys et al. [12]), rather than to work with the overall image contrast determined either by cross-variance of successive images [13], or by analyzing the intensity contained in a selected band of spatial frequencies of a single image [Wood and Krivanek, unpublished results].

Practical Considerations for Low and High Magnification Autotuning

Our strategy for practical autotuning depends on whether it is being carried out at a low or medium magnification (below about 100 000 times), or above.

At low and medium magnifications, we use a TIS-based method which proceeds in the sequence described below (the number of images needed for each step is given in brackets):

a) Complete TIS autotuning:

i) The microscope is focussed roughly by working out the defocus that minimizes image shift as the beam is tilted to two different values of $\underline{t}$ at two different values of defocus. (4)

ii) The current center $\underline{t}_c$ is determined by analyzing the shift between images taken with $\underline{t} = 0$ at two different values of focus, together with the images recorded in step (i). (2)

iii) The calibration matrices **F**, **G**, **H** and **R** are determined using different f, g, and h settings at 2 beam tilt values each. (9)

iv) The microscope is focussed and stigmated by finding the f, g, and h values that minimize the term in the square bracket in equation [3], using data obtained in the previous step. (0)

v) The focus is changed from the Gaussian defocus value worked out in step (iv) to a maximum sharpness value,

either by acquiring and analyzing a through-focus series, or simply by underfocusing by the amount required to reach Scherzer defocus. (10 or 0)

b) Focus and astigmatism correction:
vi) The microscope focus and stigmator adjustment is fine-tuned by taking 3 images with different beam tilts and solving [3] for $\underline{s} = 0$ using the calibration derived in step (iii). (3)
vii) Step (v) is repeated. (10 or 0)

All image shifts are determined by locating the maximum in a cross-correlation worked out using the Fast Fourier Transform (FFT) short-cut [1]. Determining the final focus using the sharpness maximization method results in the optimum defocus independently of whether the specimen was mostly an amplitude or a phase object, and has the further advantage that a defocus determination error due to the leakage of tilt coil field below the specimen (Fig. 2) does not influence the final result. However, the method is rather slow, so it is better to work out the needed adjustment relative to the Gaussian defocus value just once, and thereafter simply apply this value in step (v) or (vii). Similarly, the time-consuming calibrations (step iii) only need to be worked out once at each new magnification. Thereafter, only steps (vi) and (vii) need to be performed on each new specimen area, which greatly reduces the total time requirements.

Fig. 3 shows the results of TIS autotuning on a specimen of graphitized carbon imaged in a Philips CM12ST with an on-axis 1k x 1k slow-scan CCD (SSC) camera (Gatan model 679) at an electron-optical magnification of 42 000 times (on the SSC). (a) shows the misaligned and astigmatic image, (b) shows the image after rough focussing and current centering (steps i and ii), (c) after astigmatism and focus correction (step iv), and (d) after sharpness optimization (step v). Using a 256 x 256 image area and a previously worked out calibration, the focussing and stigmating that need to be carried out at each new specimen area (step iv) took 16 secs, of which 3 seconds were spent recording the three required images, and 13 seconds for calculation and communication with the microscope over an RS232 serial interface. The computer was a Macintosh IIfx with 32 MB main memory, 160 MB hard disk, an optical read-write disc using 130 MB removable cartridges, and a 20 Mflop array processor with DMA access to the main memory. All images were gain-normalized prior to the cross-correlation. This added about 2 seconds to the total processing time, but omitting the normalization produced spurious peaks at the origin of the cross-correlation. During the procedure, the images and the cross-correlation patterns were displayed on the computer monitor as soon as they were worked out, enabling the user to check the progress of the autotuning procedure.

At higher magnifications, we find that the TIS method works acceptably if there are small particles present, but is not able to work with an edge of a large particle, or a continuous amorphous film. We therefore use the ADA method, typically after a rough alignment carried out either manually or with TIS. The actual steps we employ are as follows (the number of images recorded at each step is again indicated in brackets):

a) Autoalignment:
i) Record an image, compute its diffractogram, and analyze it to determine astigmatism and defocus. (1)
ii) Adjust the defocus as needed for obtaining a diffractogram with several rings, using previously obtained calibration of the astigmatism and defocus DACs. We typically use $-(9\ C_s\ \lambda)^{1/2}$ as the defocus giving optimum diffractograms. (0)
iii) Tilt the illumination to $t_1 = (t_x, 0)$ and $t_2 = (-t_x, 0)$, where $t_x \cong 5$ mrad, and record an image at each tilt.

Fig. 3. Complete low magnification autotuning using a specimen of graphitized carbon supported on holey carbon. (a) Misaligned and astigmatic image, (b) after rough focussing and current centering, (c) after astigmatism and focus correction, and (d) after sharpness optimization.

Fig. 4. Diffractogram tableaus illustrating the tilt-induced astigmatism (TIA) autoalignment procedure. (a) Before the procedure (misalignment ≈ 4 mrad). (b) After one pass of the procedure (misalignment ≈ 0.4 mrad). (c) After a second pass of the procedure (misalignment ≈ 0.1 mrad, which is smaller than the smallest computer-controlled tilt step on the CM12).

Fig. 5. Diffractograms illustrating the automatic correction of astigmatism. (a) Before the correction (astigmatism = 53 nm). (b) After one pass of the auto-stigmating routine (astigmatism = 3 nm). (c) After a second pass of the routine (astigmatism < 1 nm).

(*Italics* again represent vectors in the complex plane.) Before commencing the tilting, adjust the defocus by $-2\ C_s\ t_x^2$, to counteract the tilt-induced defocus change. (2)
iv) Work out the existing misalignment m using the change in the apparent astigmatism of images t_1 and t_2 relative to the untilted image t_o, and set m to zero. Adjust the stigmators to set astigmatism to zero, taking account of the compensation needed for the tilt-induced astigmatism just introduced. Reset the defocus to the value it had before the autoalignment procedure started. (0)

b) Autostigmation:
v) Set defocus to the value of step (ii), take an image, and work out the astigmatism. Adjust the stigmators, and reset the focus to its previous value. (1)

c) Autofocusing:
vi) Ask the user for the desired defocus value. Record an image, compute its diffractogram, determine the focus, and adjust the focus as necessary. (1)

Step (iv) above uses the fact that with just t being varied in equation [5], the three experimentally obtained astigmatism values can be combined to give:

$$A_1 - A_2 = [(t_1 + m)^2 - (t_2 + m)^2]\ T$$

$$A_1 + A_2 - 2A_o = [(t_1 + m)^2 + (t_2 + m)^2 - 2m^2]\ T$$

Since we have chosen $t_1 = -t_2$, this simplifies to:

$$m = \frac{A_1 - A_2}{2[A_1 + A_2 - 2A_o]}\ t_1, \qquad [6]$$

where $-m$ is the tilt correction needed to bring the illumination to the coma-free axis. A_o, A_1, and A_2 correspond to, respectively, the astigmatism worked out from diffractograms recorded with no additional tilt (step i), and tilts of t_1 and t_2 (step iii).

Equation [6] shows that the mistilt in both the x and y-directions can be determined using diffractograms recorded with the tilt varying only in the x-direction. It also shows that it is important to choose the additional tilt to be large enough so that A_1 and A_2 are substantially different from A_o, and the term in the denominator does not become close to zero. Another property revealed by [6] is that because the present choice of the tilt values makes A_1 approach A_2 as correct alignment is approached, the remaining correction smoothly

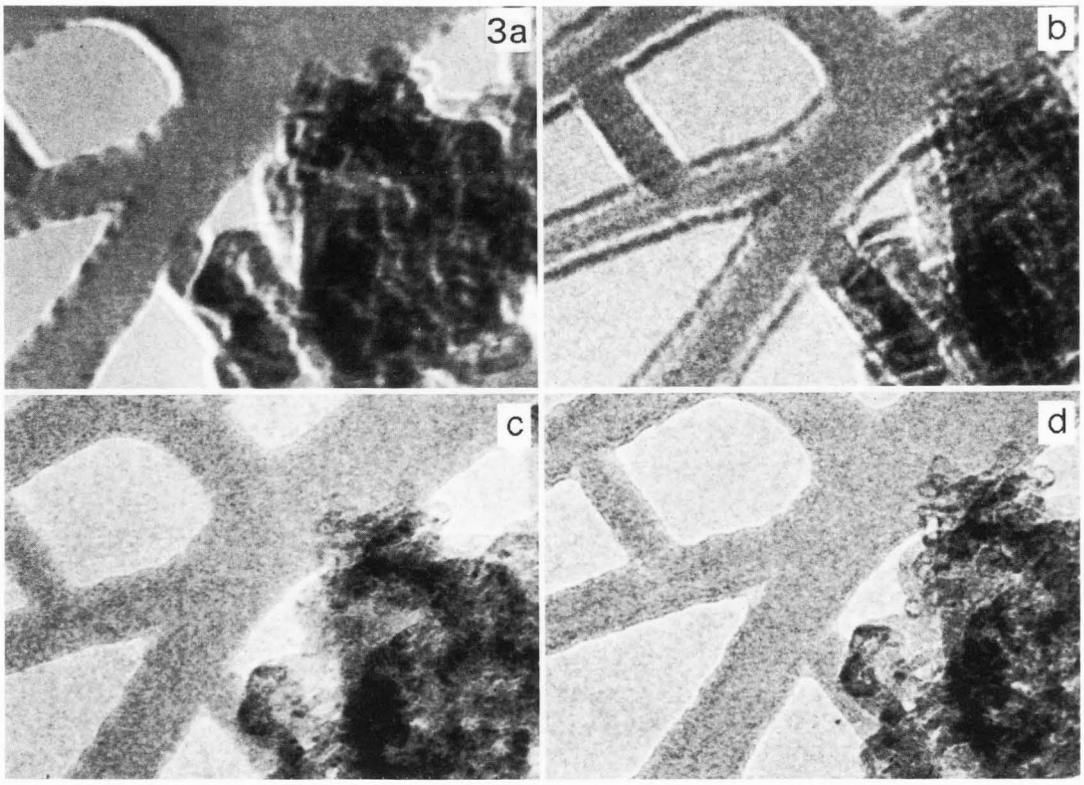
3a
b
c
d

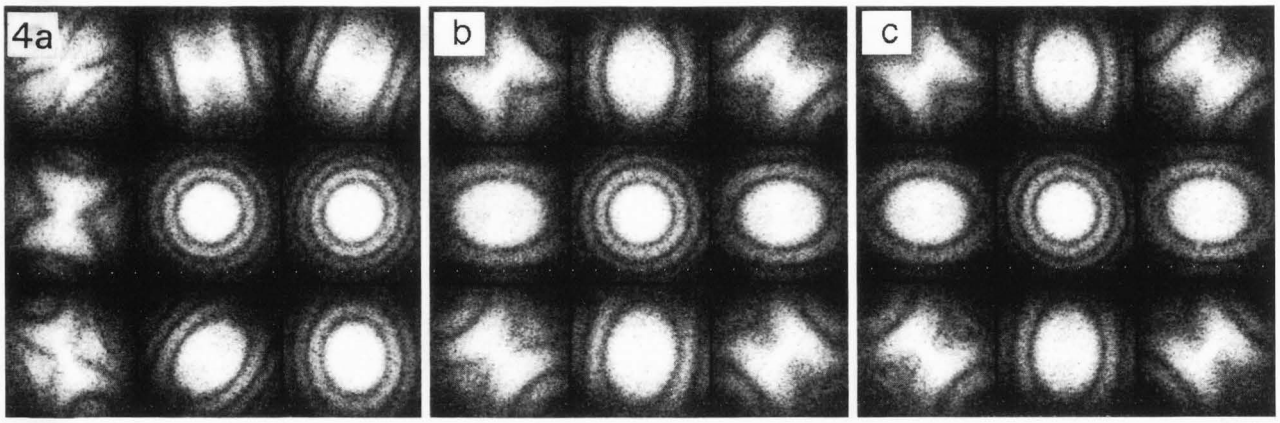
4a
b
c

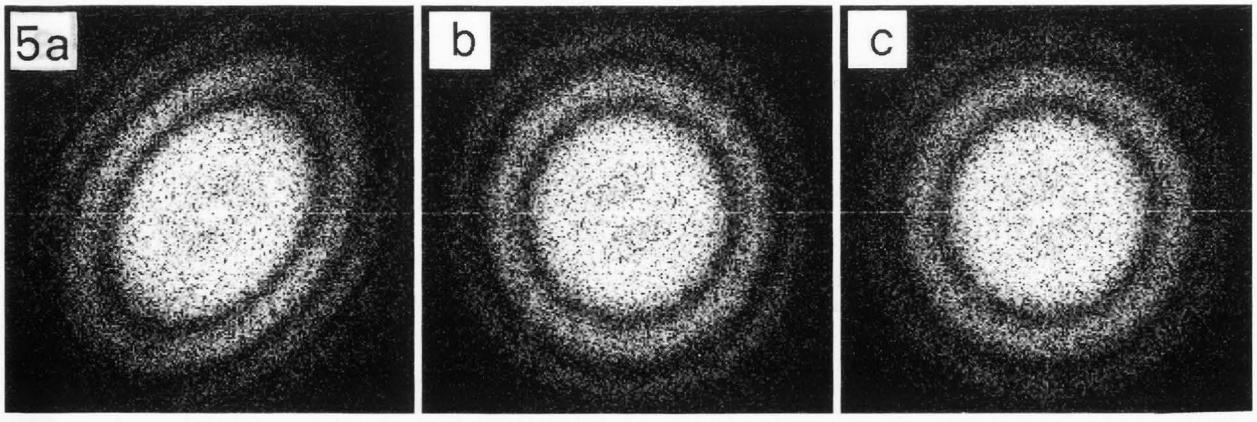
5a
b
c

tends to zero. This gives the TIA procedure stability by making it insensitive to errors such as a small miscalibration of the microscope magnification.

The above approach makes an explicit calibration of the tilt DACs unnecessary. Nevertheless, since it is useful to be able to have the computer adjust the tilt by known amounts, the software includes a routine for calibrating the tilt. The routine takes images for 3 different tilts of the illumination, and works out the tilt magnitude by fitting the resultant change in astigmatism according to equation [4b]. The stigmator and defocus computer controls are calibrated by changing the appropriate DAC, taking an image, working out the astigmatism and defocus, and comparing the new value to the value obtained before the change. Thus a total of 8 images is sufficient for a complete calibration of all the computer-controlled DACs (3 for tilt x, two more for tilt y, whose coil construction is often different from the tilt x, resulting in a different strength, and one each for astigmatism x, astigmatism y, and defocus). Moreover, the tilt and the defocus calibrations are not affected by the image rotation. Hence they tend to stay constant from session to session, provided that the same high voltage and objective lens current are used. Their values are therefore stored by the computer, and the calibration is only re-evaluated after a specific request from the user. The stigmator calibrations depend on the image rotation which typically changes when the magnification is changed, and are therefore best evaluated at the start of every autotuning session as well as after a user request.

Fig. 4 illustrates the TIA autoalignment with three diffractogram tableaus. The tableaus were obtained from a thin amorphous carbon film imaged at 120 kV in a Philips CM12ST TEM, using a side-entry 576 x 384 pixel SSC (Gatan model 689) and an electron-optical magnification of 141 000 times (on the SSC). All images were gain-normalized to avoid spurious contributions to the diffractograms due to the fixed gain pattern of the camera. In each tableau, the central diffractogram corresponds to the starting condition of corrected apparent astigmatism and possible misalignment. The surrounding diffractograms were obtained with additional tilt, whose magnitude corresponds to the distance of each diffractogram from the central one. (a) shows the diffractogram tableau before autoalignment. The diffractograms on the opposite sides of the center are substantially different from each other, demonstrating that there was appreciable misalignment (about 4 mrad). (b) shows the tableau after one pass of TIA autoalignment. The remaining misalignment is about 0.4 mrad, and the diffractograms on the opposite sides of the center are similar. (c) shows the tableau taken after one more pass of the autoalignment procedure. The remaining misalignment is about 0.1 mrad, and the opposing diffractograms are almost identical. 0.1 mrad is less than the minimum tilt change that can be produced by the computer over the RS232 interface, which is about 0.15 mrad on the CM12. Further autoalignment passes produced no additional tilt adjustment.

Each autoalignment pass took 28 seconds, of which 3 seconds were spent recording the required three images, and the rest on communicating with the microscope, calculation, and the display of the results. These times were obtained using the central 256 x 256 pixels of the SSC, and a Macintosh IIfx computer equipped with a 20 Mflop array processor. Using a Macintosh Quadra without an array processor, the total autotuning time is expected to be about the same (the Quadra takes 2 seconds per 256 x 256 Fast Fourier Transform compared to the array processor's 0.2 seconds, but is faster than the IIfx doing all the other manipulations). For a Quadra equipped with the array processor, the autoalignment is expected to take about 20 seconds. The accuracy of the procedure is typically 10% of the starting misalignment or 0.1 mrad, whichever is greater.

The autoalignment procedure needs to be carried out typically only once per high-resolution session, or if the specimen height has been changed. Further adjustments of the microscope set-up can then be carried out at the same magnification by recording and analyzing just one diffractogram, which is sufficient to correct the astigmatism, and to set the defocus to the user-selected value.

Fig. 5 illustrates the autostigmation procedure. (a) shows the diffractogram corresponding to the starting condition. The computer analyzed the diffractogram and determined that defocus was -193 nm, astigmatism 53 nm, and astigmatism direction 46°. The stigmator DACs were then reset using the calibration obtained at start-up. Another diffractogram was recorded and analyzed (b), revealing that 3 nm of astigmatism at -2° was remaining, either because the analysis of the initial condition was in error, or because the calibration was not completely accurate. Another pass of the auto-stigmating routine was therefore made. The result showed less than 1 nm of astigmatism (c). Each pass of the procedure took 10 seconds on a Macintosh IIfx with an array processor. The accuracy of the routine is typically 10% of the previous astigmatism value or 1 nm, whichever is greater.

The full implementation of ADA autotuning takes just 3 images, and puts the microscope in a coma-free and stigmated condition, and at a user-selected defocus value. A practical disadvantage of the method is that a single bad diffractogram, for instance due to a momentary vibration, can throw it off. In order to guard against such a possibility, the software monitors the precision of the diffractogram analysis, and alerts the user when it has detected that a diffractogram fit may be seriously in error. It also computes the location of the diffractogram rings corresponding to the fitted values of defocus and astigmatism, and it superimposes the rings on each analyzed diffractogram. The user can thereby judge visually the quality of the fit, and interrupt the procedure if it is clear that the fit is not a good one. On the whole, our practical experience with ADA autotuning is that it completely takes out the mystery from HREM alignment, stigmation, and focusing, making itself invaluable to experts and novices alike.

Since our aim is to make autotuning available on all existing types of high resolution electron microscopes, we have separated the microscope-dependent part from the main body of the software. In this approach, the autotuning software calls a separate microscope control routine (implemented as a CustomFunction within DigitalMicrograph) whenever it needs any microscope parameter changed, and there is one control routine for each type of a microscope. This simplifies the autotuning code considerably. The control routines we have written so far are able to control 5 different types of electron microscopes, including two which did not have digital interfaces, and therefore had to be fitted with external digital-to-analog (D/A) converters and associated electronics. All 5 types of microscopes could be autotuned, showing that the ADA and TIS methods described above have a general validity.

Other Uses of Slow-Scan CCD Cameras for On-Line Microscope Control

Slow scan CCD cameras are also highly useful for quantitative image analysis and processing, quantitative electron diffraction, electron holography, 3D reconstruction, and high-resolution EM (see reference [11] for an overview of recent SSC applications). In most of these procedures the amount of on-line control of the microscope by the computer is minimal, but there a few exceptions.

One application in which the SSC is used in conjunction with microscope control by the computer is image splicing as needed for recording images larger than the size of the CCD sensor [4]. Here the computer controls image deflection coils,

and shifts the image on the CCD sensor to produce a tableau of slightly overlapping images. It then works out the precise image shift by doing cross-correlation of the overlapping image parts. As a final step, it "splices" together the partial images to produce one larger image.

Another application is low-dose microscopy using the spot-scan method [2]. Here the computer controls both the image and illumination deflection coils, and uses them in a precise ratio such that the illuminating spot on the specimen and the image position on the CCD sensor are shifted so that each new image registered on the CCD corresponds to a freshly exposed area on the specimen. The shift needs to be precisely calibrated, because the images are again spliced together to form one larger image, but this time typically without the benefit of overlapping image parts. The method has the advantage that only a small specimen area is illuminated at any one time, thereby minimizing specimen shrinkage [2].

Conclusion

Predictive TEM autotuning methods benefit from the high quality of input data provided by slow-scan CCD cameras. The tilt-induced image shift (TIS) method of Koster, van der Mast and de Ruijter is a robust procedure which can adjust the microscope from a long way off, and works especially well at low and medium magnification. The automated diffractogram analysis (ADA) method introduced in this paper works only at high magnification with images of amorphous materials, and requires the starting condition to be good enough to give diffractograms with at least two rings. Within its domain of validity, however, it is simpler, faster, more precise, and less prone to artifacts than any other presently known TEM autotuning method. A combination of TIS and ADA works well at both low and high magnifications, and opens up the prospect for autotuning to become as popular in transmission electron microscopy as it already is in the world of 35-mm film cameras.

Acknowledgements

We are grateful to Hans de Ruijter for sending us a copy of reference [6] prior to publication and for a critical reading of the manuscript, and to Mike Leber and Chris Meyer for help with software implementation.

References

[1] Bracewell RN (1986). The Fourier Transform and Its Applications. (McGraw-Hill, New York), p. 46.

[2] Downing KH (1991). Spot-Scan Imaging in Transmission Electron Microscopy. Science **251**, 53-59.

[3] Fan GY and Krivanek OL (1990). Computer-controlled HREM alignment using automated diffractogram analysis. Proc. 12th Int. Congr. on Electron Microscopy, Seattle, Peachey LD, Williams DB (eds.) (San Francisco Press, San Francisco), **1**, 332-333.

[4] Fan GY, Gubbens AJ, Krivanek OL, Leber ML and Mooney PE (1991). Combining slow-scan CCD images to extend image size and dynamic range. Proceedings 49th EMSA meet., Bailey GW (ed.) (San Francisco Press, San Francisco), 524-525.

[5] Koster AJ, van den Bos A and van der Mast KD (1987). An autofocus method for a TEM. Ultramicroscopy **21**, 209-221.

[6] Koster AJ and de Ruijter WJ (1992). Practical Autoalignment of Transmission Electron Microscopes. Ultramicroscopy **40**, 89-107.

[7] Koster AJ, van den Bos A and van der Mast KD (1988). Signal processing for autofocusing by beam tilt induced image displacement. Scanning Microscopy Supplement **2**, 83-92.

[8] Krivanek OL (1976). Determining the coefficient of spherical aberration from a single electron micrograph. Optik **45**, 97-101.

[9] Krivanek OL (1978). EM contrast transfer functions for tilted illumination imaging. Proc. 9th Int. Congr. on Electron Microscopy, Sturge JM (ed.) (Microscopical Society of Canada, Toronto), **1**, 168-169.

[10] Krivanek OL, Stadelmann P, Higgs A, Chen C and Disko MM (1983). Is full automation of HREM feasible? Proceedings 41st EMSA meet., Bailey GW (ed.) (San Francisco Press, San Francisco), 404-405.

[11] Krivanek OL, Mooney PE, Fan GY, Leber ML and Meyer CE (1991). Slow-scan CCD cameras for Electron Microscopy. Inst. Phys. Conf. Ser. **119**, 523-526.

[12] Nys B, Geuens I, Naudts J, Gijbels R, Jacob W and Van Espen P (1990). A convenient method for autofocusing based on information content. J. Computer-Assisted Microscopy **2**, 115-123.

[13] Saxton WO, Smith DJ and Erasmus SJ (1983). Procedures for focusing, stigmating and alignment in high resolution electron microscopy. J. Microscopy **130**, 187-201.

[14] Smith DJ, Higgs A and Perkes P (1987). Practical experience with computer-controlled high-resolution electron microscopy. *In*: Proceedings 45th EMSA meet., Bailey GW (ed.) (San Francisco Press, San Francisco), 62-65.

[15] Spence JCH (1981). Experimental high resolution electron microscopy. (Clarendon Press, Oxford), p. 83.

[16] van der Mast KD (1984). Automizing electron microscopes. Proc. 8th European Congr. on Electron Microscopy, Budapest, Csadany A, Rohlich P and Szabo D (eds.) (Hungarian Group for Electron Microscopy, Budapest), **1**, 3-9.

[17] Zemlin E, Weiss K, Schiske P, Kunath W and Herrmann K-H (1978). Coma-free alignment of high resolution electron microscopes with the aid of optical diffractograms. Ultramicroscopy **3**, 49-60.

Discussion with Reviewers

P. Rez: How large is the area of amorphous carbon film needed for the ADA method?
Authors: The main requirement of the method is that there be a recognizable diffractogram with at least 2 distinct rings. Because the quality of a diffractogram depends heavily on factors such as the brightness of the electron source and the nature of the sample, we have not done a systematic investigation of just how small a specimen area can produce a suitable diffractogram. However, we have been able to use a 30 - 50 Å wide contamination layer on the edge of a crystalline specimen, and we therefore suspect that the minimum usable specimen area is around 30 Å in diameter.

P. Rez: What would the authors propose for autotuning with crystalline specimens?
Authors: If there is a contamination layer on the sample, it might be possible to isolate its contribution to a diffractogram by placing an upper threshold on allowed diffractogram intensity, so as to filter out the Bragg beams. If there is no contamination layer, putting a small patch of amorphous carbon somewhere on the sample might be the solution. Another approach might be to use the crystalline image in a modified TIS method in which the shift of different spatial frequencies is monitored separately (de Ruijter WJ, Rez P and Smith DJ, Proc. 12th Int. Congr. on Electron Microscopy, Seattle, Peachey LD, Williams DB (eds.) (San Francisco

Press, San Francisco), **1**, 154-155). However, such a method would suffer from the problems encountered by TIS when it is applied at very high magnification (see below).

P. Rez: It is now possible to build a system that can update a tableau of 5 diffractograms once every second. With the aid of such a tableau even inexperienced users should have no difficulty in setting the focus, astigmatism and beam tilt. Would the authors like to comment on the necessity of "closing the loop" and automating the process as described in this paper?
Authors: The on-line tableau method is valuable, but complete autotuning has many of the advantages that typically follow when a manual procedure is completely automated: 1) it is more reproducible and typically more accurate (as found for instance by high resolution microscopists at Arizona State University), 2) it can be done faster, thus saving time and minimizing irradiation of the sample (note that no irradiation needs to take place while the computer is evaluating the results), 3) it can be used in complicated procedures that would be unbearably tedious to a human user, e.g. automatically refocusing each time a new tilt is reached in a 3-D reconstruction procedure involving say 100 different projections, or taking a large through-focus series and checking for the correct defocus value at every step.

H. Tietz: Have the authors investigated the relative accuracy and reproducibility of the TIS and ADA methods under instrumental and specimen conditions where both methods could be used?
Authors: As stated in the paper, ADA does not work at low magnifications, and also needs amorphous specimens. On the other hand, ADA is not thrown off by practical factors such as specimen drift and defocus drift, which typically limit the accuracy of TIS at very high magnifications. Further, ADA only needs a single micrograph for focusing and stigmating, and 3 micrographs for complete autotuning, whereas TIS needs about twice as many micrographs to perform the same tasks. It is therefore our opinion that the TIS and ADA methods have fairly separate domains of usefulness, and we have not done a systematic comparison. Nevertheless, we expect that once both methods become generally available to users, it will not take long before their relative merits are firmly established.